

Simulating a Manufacturing System including an Air Compressor for Reducing Energy Costs

Vansh Vyas, Hyun Woo Jeon, Louisiana State University, LSU-IAC

ABSTRACT

Generally, the manufacturing industry's electricity cost is calculated as the summation of energy charge (total kWh \times \$/kWh) and demand charge (peak kW \times \$/kW). Thus, one possible way for sustainable and cost-efficient manufacturing is to reduce kWh consumption or peak kW. A compressed air system (CAS) is one of the most energy-consuming and commonly used systems in manufacturing since it supports manufacturing processes and other auxiliary systems. Even though some preliminary studies on energy consumption of a CAS and machining process are available, existing research studies are not comprehensive in integrating power loads of both a CAS and production system. This paper, therefore, proposes an electrical load simulation tool integrating a CAS and machine-level power demand to estimate the factory level power demand and energy consumption by using simulation techniques. Further, this tool considers a rotary screw air compressor with start/stop mode and available turning machine power demand model for energy simulation. Thus, the resulting simulation analysis from this study will help manufacturers have a better understanding of energy consumption in their manufacturing systems to reduce peak demand, energy consumption, and energy-related costs by finding the optimized settings for a CAS and production schedule. This study will also contribute to the reduction of carbon footprint by improving energy efficiency in manufacturing systems. With the help of 20 case studies, we found that the significant factors affecting the energy cost are the magnitude of compressed air leakage, discharge pressure, machine-level compressed air consumption, and the variability of machine processing time.

1. Introduction

Economic and environmental sustainabilities are largely affected by the industrial sector. The industrial sector itself accounts for about 32% of the total energy consumption in the United States ("U.S. Energy Information Administration (EIA)" 2019). So, to improve the energy efficiency of a production system, manufacturers must understand the dynamics of the energy consumption in their facilities. In general, the electricity cost for manufacturers consists of two charges: (i) an energy charge based on kWh consumption (kWh \times \$/kWh) and (ii) a demand charge based on the peak energy demand (kW \times \$/kW). Therefore, one possible way for manufacturers to practice sustainable and cost-efficient manufacturing is to reduce their kWh consumption or peak kW. Various studies have been conducted to evaluate these electrical charges. For example, the study by Wang and Li (2015) shows a detailed survey of the energy consumption charge and the demand charge for industrial customers in the U.S. The study concludes that electricity cost savings can vary enormously when customers transition from flat rates to time of use pricing depending on specific utility programs and production strategies.

Over time, researchers have focused on the operational perspective of the production system and have investigated the minimization of its energy consumption. In particular,

machining processes such as milling and turning that involve material removal have been found to contribute significantly towards energy consumption (Li et al. 2015). Additionally, simulation approaches of discrete-event simulation (DES) and numerical simulation have been used to estimate machine-level power demand for various material removal processes (Jeon, Lee, and Wang 2019; Jeon et al. 2017). A compressed air system (CAS) is one of the most energy-consuming systems in manufacturing (Saidur, Rahim, and Hasanuzzaman 2010). A CAS, however, has not been studied comprehensively with a production system involving machining processes to investigate the facility level energy consumption. This lack of studies suggests that there is a need to consider the integration of a CAS and machine-level energy demand to evaluate the effects of various CAS and machine-level parameters on facility-level energy parameters.

2. Background

In manufacturing industries, a CAS is one of the most commonly used systems since it supports a variety of pneumatic tools and production processes (CAGI 2016). Additionally, a CAS is one of the most energy-consuming equipment and accounts for about 10% of the total electricity consumption in the U.S. (Senniappan 2004). Generally, a CAS consumes about 5% to 20% of the facility's annual electricity cost (Schmidt and Kissock 2005), and 20-50% of energy can be saved by improving a CAS (Shanghai and McKane 2008). Hence, it is beneficial for the manufacturers to understand the energy consumption of a CAS to reduce their energy costs.

A CAS includes the air supply and demand side. The air supply side includes various equipment responsible for supplying compressed air such as the air compressor and the air receiver (LBNL and RDC 2003). The air demand side includes various equipment that consumes compressed air such as machines and pneumatic tools (LBNL and RDC 2003). Out of all the compressor types, the rotary screw, reciprocating, and centrifugal compressors are three of the most commonly used CAS in manufacturing industries (CAGI 2016; LBNL and RDC 2003; Schmidt and Kissock 2003). Generally, a CAS is equipped with various control modes for an efficient operation to match the supply and demand (LBNL and RDC 2003). The most common CAS control modes are start/stop, load/unload, inlet modulation, dual-control, variable displacement, and variable speed controls (Compressed Air Challenge 2002). For our study, we will choose a rotary screw air compressor working on the start/stop control mode as it is one of the most commonly used systems (LBNL and RDC 2003). In a CAS equipped with the start/stop control mode, the driving motor turns on or off based on the start and stop pressure settings. More specifically, a CAS supplies the compressed air until the discharge pressure is met (start mode), and the air compressor motor remains turned off until the system pressure drops to a preset pressure level (stop mode). Consequently, a CAS with the start/stop control mode is equipped with an air receiver to have a constant pressure supply during the stop mode (LBNL and RDC 2003).

The average power required by the air compressor (W_{CAS}) is defined as the amount of power required to operate the air compressor during its operation time and can be calculated using available formulas. A CAS equipped with the start/stop control mode would consume power only during the start mode, and the power requirement for a CAS is zero during the stop mode (LBNL and RDC 2003). So, W_{CAS} depends on the average power required by a CAS

during the start mode and can be calculated as:

$$W_{CAS} = H_R \times B_{CF} \times (1/E_m) \times R_{HP} \times R_{Start} \quad (1)$$

where,

H_R = rated horsepower (HP) of the air compressor,

B_{CF} = conversion factor to convert HP to kW = 0.746 kW/HP,

E_m = efficiency of the air compressor motor,

R_{HP} = proportion of H_R required by a CAS during the start mode, and

R_{Start} = proportion of the time a CAS is running in the start mode (LBNL and RDC 2003).

According to LBNL and RDC (2003), the full-load power or the power required during the start mode of a CAS can be estimated as 10% above H_R or 110% of H_R ($R_{HP} = 1.10$).

The fundamental equation governing the dynamics of the air receiver is given as:

$$t_P = (V \times |P_{final} - P_{initial}|) / (F_R \times P_a) \quad (2)$$

where,

t_P = time to fill or empty the air receiver (minutes),

V = size of the air receiver (cubic feet),

P_{final} = final air receiver pressure (psig),

$P_{initial}$ = initial air receiver pressure (psig),

F_R = compressed air supply or demand flow rate (cubic feet per minute (cfm)), and

P_a = absolute atmospheric pressure (psia) = 14.7 psia (CAGI 2016).

The time duration for the start mode (t_{Start}) and stop mode (t_{Stop}) respectively can be estimated using the fundamental equation governing the dynamics of the air receiver. For the start mode, t_P (Eq. (2)) can be modified as:

$$t_{Start} = (V \times (P_{Stop} - P_{initial})) / ((S - C) \times P_a) \quad (3)$$

where,

t_{Start} = the time duration to reach the discharge pressure during the start mode of a CAS (min),

P_{Stop} = discharge pressure, that is, pressure at which the air compressor motor stops (psig),

S = compressed air flow rate (supply) from the air compressor to the air receiver (cfm), and

C = total compressed air flow rate (demand) from the air receiver to the equipment (cfm).

For the stop mode, t_P (Eq. (2)) can be modified as:

$$t_{Stop} = (V \times (P_{initial} - P_{Start})) / (C \times P_a) \quad (4)$$

where,

t_{Stop} = the time duration for the pressure drop to continue till the pressure in the air receiver reaches the preset pressure level during the stop mode of a CAS (min), and

P_{Start} = pressure at which the air compressor motor starts again (psig).

Additionally, the compressed air flow rate from the air compressor (S) is significantly impacted by the discharge pressure (P_{Stop}) (Downs 2020). Generally, S at a given P_{Stop} is provided by the manufacturer of the air compressor. For calculation purposes, S at different P_{Stop} can be estimated using Boyle's law as:

$$S = (S_R \times (P_{Stop})_R) / P_{Stop} \quad (5)$$

where,

S_R = manufacturer rated compressed air flow rate from the air compressor at the rated discharge pressure (cfm), and

$(P_{Stop})_R$ = manufacturer rated discharge pressure (psig) (Downs 2020).

To identify potential energy savings opportunities in a CAS, various researchers have thoroughly studied the energy consumption of a CAS (Saidur, Rahim, and Hasanuzzaman 2010). Various studies suggest that the manufacturers can achieve large energy savings by making small modifications in a CAS (Saidur, Rahim, and Hasanuzzaman 2010). Few modifications that can reduce the energy cost of a CAS are reducing compressed air leaks, reducing discharge pressure, matching supply with demand, and using a high-efficiency motor (Saidur, Rahim, and Hasanuzzaman 2010; LBNL and RDC 2003). Also, researchers have developed a method to estimate the operating efficiency of a CAS for different control modes (Schmidt and Kissock 2003). Further, the study concludes that potential problems such as inadequate compressed air storage, over-sized compressors, and compressed air leaks can be identified based on the CAS power signatures. To estimate energy consumption of a CAS, researchers have also used simulation software that uses actual CAS power data (Schmidt and Kissock 2005). The researchers found that the type of compressor control and proper compressor sizing are important factors that affect the energy cost of a CAS. Moreover, improper sizing of a CAS and inefficient CAS control modes can increase the operating costs of a CAS (Schmidt and Kissock 2005).

Based on the thermal equilibrium, a processing rate has been identified as the main component of an energy model (Gutowski et al. 2009). To evaluate the energy consumption associated with the material removing processes such as milling and turning, various energy models have been developed. Kara and Li (2011) developed an empirical model to predict the energy consumption for the material removal process such as milling or turning based on the material removal rate (MRR). Researchers have also considered the dependence of various production parameters such as spindle speed and cutting speed to experimentally evaluate the mathematical models to optimize the energy consumption of the material removal process (Kara and Li 2011; Vechev et al. 2014). Various studies have considered machining power as a linear function of MRR as power (kW) \approx (idle power of the machine) + (specific energy consumption) \times MRR to estimate the power demand of the material removal processes such as milling and turning (Diaz, Redelsheimer, and Dornfeld 2011; Herrmann et al. 2011; Jeon et al. 2017; Jeon and Lee 2016). Simulation approaches have also been used by various studies to estimate machine-level power demand and energy costs. For example, a simulation approach to estimate the power demand for various manufacturing processes such as milling and turning was proposed in the study by Jeon, Taisch, and Prabhu (2016). Additionally, simulation techniques of DES and numerical simulation have been used with copula models to check the effects of production parameters on energy costs (Jeon, Lee, and Wang 2019).

The studies related to a CAS and machining energy consumption are available separately. However, the combined effects of a CAS and machining parameters on energy performances have not been studied well enough for the opportunities of reducing and saving energy cost especially when simulation approaches are applied. As a CAS is one of the most energy-consuming equipment in the manufacturing system, a simulation model needs to be built so that the power demands of both a CAS and machining processes can be integrated. To address such a research gap, this study proposes a power demand simulation model combining a CAS and machines to evaluate the impact of machining and CAS parameters on peak kW, energy consumption, and energy costs at the factory level. Such a system can be modeled using a combination of two simulation techniques: (i) DES and (ii) numerical simulation. The simulation model can be developed with the help of DES by sequencing events at discrete time intervals. Further, mathematical models for a physical system can be incorporated into computer software for numerical simulation. We will consider various CAS and machining parameters such as the magnitude of compressed air leakages, discharge pressure, and variability in processing time to make the model realistic. Further, with the help of several simulation cases, we will show how various CAS and machine-level parameters affect energy performances. Since the power profile of any system is continuous, it is hard to determine the system power at a given time. Therefore, the electricity providers in the U.S. calculates the peak kW by metering the power at an interval of 15 min, 30 min, or 60 min (Wang and Li 2015). Hence, we believe that an average of metering intervals (moving average) can be used to estimate the peak kW. With the help of the proposed model, the manufacturers can study and evaluate the power demand of the facility to reduce their energy cost by optimizing a CAS or machining parameter. Additionally, the manufacturers can test the effects of different CAS and machining parameters on the energy performances before applying them to a real system. Moreover, this tool can be useful for academic practitioners and manufacturers to study the time-series power demand. For example, the manufacturers can study the power data and adapt various peak shaving methods to reduce their peak kW.

The rest of the paper is organized as follows. Section 3 presents a simulation-based model to estimate the power demand of the facility. The results and discussions from relevant simulation examples based on our proposed simulation model are provided in Section 4. In Section 5, the conclusions of the findings from the study and potential topics for future research are presented.

3. Power Demand Simulation Model

This section provides a simulation model to estimate the peak value of the 15-min moving average for the power demand and energy consumption of the facility by integrating a CAS and machine-level power demand.

3.1 Estimation of Power Consumption of a CAS Working on Start/Stop Mode

The power (kW) required by a CAS during start mode (W_{Start}) can be estimated as 110% of H_R (LBNL and RDC 2003). A CAS requires almost no power during stop mode based on the reference (LBNL and RDC 2003) and our collected power data. So, we estimate the power

required by a CAS during stop mode (W_{Stop}) is zero ($W_{Stop} = 0$). Moreover, a CAS only consumes power during the start mode and we propose the following estimate for W_{Start} :

$$W_{Start} = (H_R) \times (B_{CF}) \times (1/E_m) \times 1.10 \quad (6)$$

Since $W_{Stop} = 0$, the average power required by a CAS (W_{CAS}) will only depend on the average power required by a CAS during start mode, and W_{CAS} can then be estimated based on the reference as (LBNL and RDC 2003):

$$W_{CAS} = (W_{Start} \times R_{Start}) = (H_R) \times (B_{CF}) \times (1/E_m) \times 1.10 \times R_{Start} \quad (7)$$

R_{Start} can be estimated using the power profile of a CAS as the ratio of the total time that a CAS runs in the start mode to the total operational time of a CAS.

3.2 Pressure-Discretized Algorithm to Estimate a CAS Power Profile

To obtain the power profile of a CAS with start/stop control as shown in Figure 1, we need time-series power demand data for a CAS. To generate the time-series power demand data for a CAS, we need four parameters: the power required by a CAS during the start mode (W_{Start}), the power required by a CAS during the stop mode (W_{Stop}), the time duration to reach the discharge pressure during the start mode of a CAS (t_{Start}), and the time duration to reach the starting pressure during the stop mode of a CAS (t_{Stop}) (see Figure 1). W_{Start} can be estimated from equation (Eq.) (6), W_{Stop} can be estimated as zero, and t_{Start} and t_{Stop} can be estimated from the eqs. provided in Section 2. Further, we can estimate R_{Start} using the time-series power data for a CAS once it is generated. Then, once the power profile of a CAS is created, we can estimate W_{CAS} , the peak value of the 15-min moving average (MA) for CAS power demand (P_kW_{15}), and the total kWh consumption for a CAS.

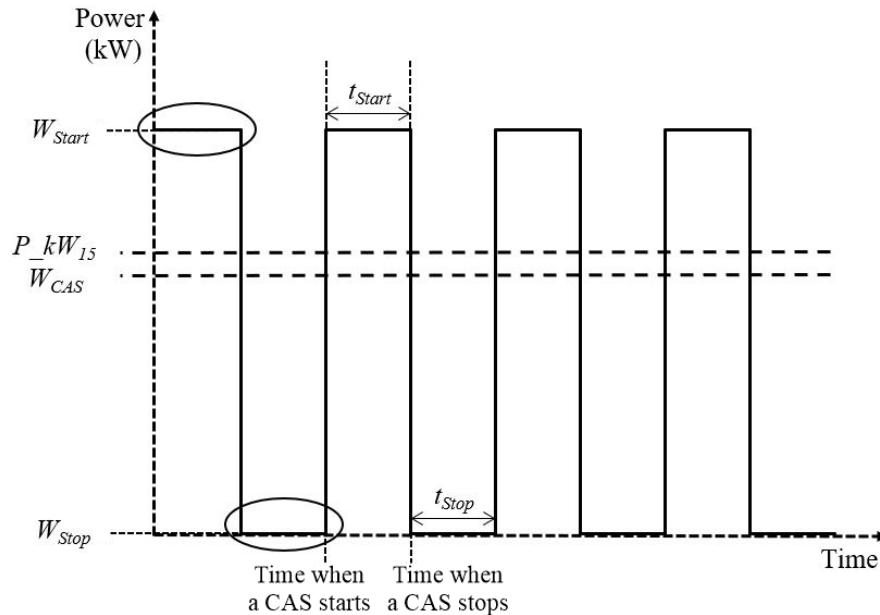


Figure 1. The estimated power profile of CAS with start/stop controls

To obtain the power profile of a CAS, we will develop a model that can replicate the working of a CAS. To do so, we will develop an algorithm to change the pressure inside the air receiver by small units for the start and stop modes of a CAS. More specifically, we will discretize the pressure range into equal fragments of 0.5 psig as shown in Figure 2. Further, we will define the time duration (t) for 0.5 psig pressure change to occur for the start and stop mode based on the eqs. for t_{Start} (Eq. (3)) and t_{Stop} (Eq. (4)) as follows:

$$t = (0.5 \times V) / [(S - C_i) \times 14.7] \text{ (for start mode)} \quad (8)$$

$$t = (0.5 \times V) / (C_i \times 14.7) \text{ (for stop mode)} \quad (9)$$

where,

t = time duration for the pressure to rise (start mode of a CAS) or drop (stop mode of a CAS) by 0.5 psig and

C_i = total compressed air demand at i^{th} time.

In Eqs. (8) and (9), we will fix V and S and additionally, we will define all the air demand requirements in the model. Then, the pressure inside the air receiver during the start and stop mode will be updated after the defined time duration (Eqs. (8) and (9)) as:

$$P_i = P_{i-1} + 0.5 \text{ (for start mode)} \quad (10)$$

$$P_i = P_{i-1} - 0.5 \text{ (for stop mode)} \quad (11)$$

where,

P_i = pressure inside the air receiver at i^{th} time and

P_{i-1} = pressure inside the air receiver at $(i-1)^{\text{th}}$ time.

Figure 3 shows the detailed summary of the algorithm to estimate the pressure inside the air receiver at any given time.

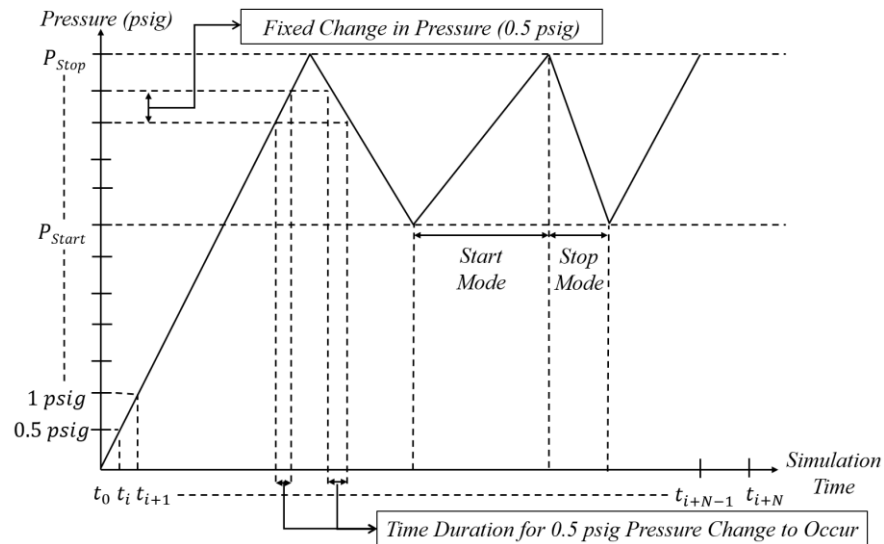


Figure 2. Discretization of pressure

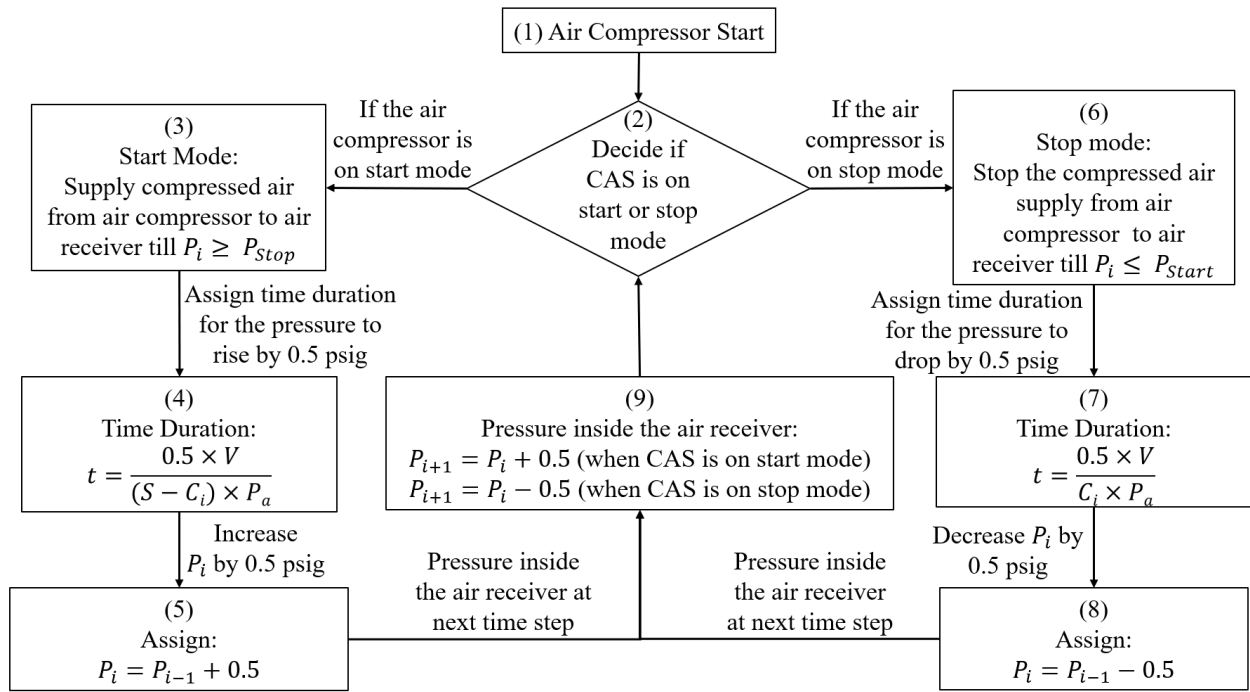


Figure 3. Algorithm to estimate CAS pressure

3.3 Machine-Level Power Demand Estimation

The basic power equation for any material removing process is estimated as a linear function of MRR (processing rate (A) / processing time (T)) and can be estimated as:

$$W \approx b_2 + b_1 \times \text{MRR} \approx b_2 + b_1 \times A / T \quad (12)$$

where,

W = machine-level power (W),

b_2 = idle power of the machine (W), and

b_1 = specific energy consumption ($\text{W} \times \text{min}/\text{mm}^3$) (Diaz, Redelsheimer, and Dornfeld 2011; Herrmann et al. 2011; Jeon et al. 2017; Jeon and Lee 2016).

For this study, we will consider a set of turning machines and use turning parameters (as shown in Table 1) to estimate the power demand at the machine level.

Table 1. Turning parameters for different materials

| Serial No. | Material name | MRR | | Avg. A (mm^3) | Avg. T (min) | Power eq. param. | | Avg. W |
|------------|-----------------|----------------------------------|----------------------------------|----------------------------|----------------|--|-----------|----------|
| | | min (mm^3/min) | max (mm^3/min) | | | b_1 ($\text{W} \times \text{min}/\text{mm}^3$) | b_2 (W) | |
| 1 | Alloy cast iron | 33,717 | 119,881 | 767,990 | 10 | 0.0137 | 2,596.6 | 3,646 |
| 2 | Aluminum alloys | 80,742 | 384,882 | 2,328,123 | 10 | 0.0113 | 2,596.6 | 5,235 |
| 3 | Brass | 84,292 | 283,929 | 1,841,105 | 10 | 0.0377 | 2,596.6 | 9,531 |
| 4 | Bronze | 71,180 | 239,763 | 1,554,711 | 10 | 0.0377 | 2,596.6 | 8,453 |
| 5 | Cast steel | 24,647 | 92,425 | 585,358 | 10 | 0.0282 | 2,596.6 | 4,245 |
| 6 | Copper | 9,390 | 281,711 | 1,455,508 | 10 | 0.0408 | 2,596.6 | 8,540 |

| | | | | | | | | |
|----|------------------------------------|--------|---------|-----------|----|--------|---------|-------|
| 7 | High carbon alloy steels | 5,767 | 202,300 | 1,040,335 | 10 | 0.0657 | 2,596.6 | 9,428 |
| 8 | High temperature nickel and cobalt | 24,844 | 24,844 | 248,438 | 10 | 0.1133 | 2,596.6 | 5,412 |
| 9 | Lead | 44,364 | 44,364 | 443,640 | 10 | 0.0100 | 2,596.6 | 3,040 |
| 10 | Low carbon alloy steels | 10,647 | 85,031 | 478,392 | 10 | 0.0497 | 2,596.6 | 4,973 |
| 11 | Magnesium alloys | 74,926 | 126,191 | 1,005,583 | 10 | 0.0122 | 2,596.6 | 3,820 |
| 12 | Malleable iron | 37,562 | 153,795 | 956,783 | 10 | 0.0190 | 2,596.6 | 4,414 |
| 13 | Medium carbon alloy steels | 4,880 | 79,485 | 421,827 | 10 | 0.0612 | 2,596.6 | 5,177 |
| 14 | Monel | 13,309 | 13,309 | 133,092 | 10 | 0.0453 | 2,596.6 | 3,200 |
| 15 | Plain cast iron | 55,455 | 131,613 | 935,341 | 10 | 0.0137 | 2,596.6 | 3,875 |
| 16 | Steels | 5,915 | 8,873 | 73,940 | 10 | 0.0633 | 2,596.6 | 3,065 |
| 17 | Titanium Alloys | 6,729 | 153,376 | 800,523 | 10 | 0.0543 | 2,596.6 | 6,946 |
| 18 | Zinc alloys | 98,587 | 98,587 | 985,866 | 10 | 0.0113 | 2,596.6 | 3,714 |

Modified from a source. *Source:* Kara, S., and W. Li. 2011. "Unit Process Energy Consumption Models for Material Removal Processes." *CIRP Annals - Manufacturing Technology*, no. 60: 37–40.

3.4 Factory Level Power Demand Estimation

To estimate the factory-level power demand, we need a model that is capable of integrating the actual power demands from a CAS and machines. To actualize such a model, simulation methods of discrete-event simulation (DES) and numerical simulation can be used. Further, we will develop a pressure-discretized energy simulation model to estimate the power required by the air compressor and the available machine-level power demand models by using the simulation methods. Then, the integration of the power required by a CAS and machines will determine the factory level power. We will use software such as Simio (for DES) and MATLAB (for numerical simulation) to develop such a model. We will design the production layout with a CAS and machines using the objects provided in Simio. The simulation model will consist of the air supply and air demand-side. The operational parameters of a CAS such as the pressure setpoints (P_{Start} and P_{Stop}), the size of the air receiver (V), and the compressed air flow rate from the air compressor to the air receiver (S) will be defined at the air supply-side. For the air-demand side, we will define the machine processing time, product flow, machine-level compressed air demand, and the total magnitude of compressed air leakages. Additionally, we will define the time duration for the pressure to update in the air receiver by 0.5 psig for the start and stop modes of a CAS. Furthermore, we will define a process in Simio to generate the set of times when a CAS works on the start and stop mode. We will then use the timestamps as an input in MATLAB along with the power estimation equations for a CAS to create the time-series power profile for a CAS. To generate the time-series power demand data for machines, we will follow an existing approach and a detailed explanation can be found in the study by Jeon, Lee, and Wang (2019). To estimate the factory level power, we will aggregate the power demand from a CAS and machines for the same timestamp. Further, the energy cost can be calculated using the peak kW and total kWh obtained from the simulation results. Figure 4 provides the summary of the factory-level power demand estimation.

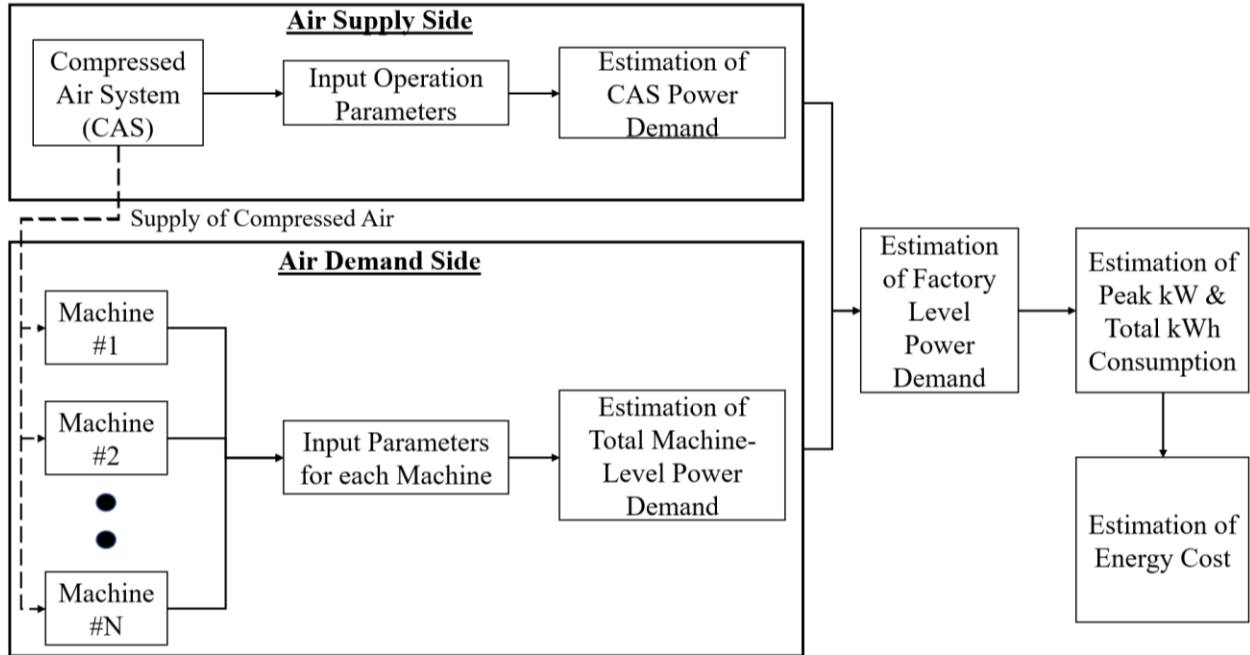


Figure 4. Summary of facility-level power demand estimation

4. Illustrative Examples & Results

This section provides the results from the simulation examples based on our proposed method.

4.1 Electricity Rate Structure

To estimate the energy cost for the simulation examples, we are using the existing demand rate (\$/kW) and total electricity consumption rate (\$/kWh) from previous studies (Wang and Li 2015; “State Electricity Profiles - Energy Information Administration (n.d.)” 2017). For our study, we chose four U.S states, Louisiana (LA), Michigan (MI), Connecticut (CT), and Hawaii (HI). We chose LA and HI since they have the lowest and highest energy consumption rate, respectively. Table 2 shows the summary of the electricity rate structures.

Table 2. Electricity rate structures

| Electricity Rate | LA | MI | CT | HI |
|------------------|--------|--------|--------|--------|
| \$/kWh | 0.0771 | 0.1140 | 0.1841 | 0.2918 |
| \$/kW | 8.56 | 5.69 | 11.96 | 19.5 |

Source: Wang, Yong, and Lin Li. 2015. “Time-of-Use Electricity Pricing for Industrial Customers: A Survey of U.S. Utilities.” *Applied Energy*, no. 149: 89–103; “State Electricity Profiles - Energy Information Administration (n.d.)” 2017.

4.2 Simulation Example Results & Discussion

In our production system simulation model, we assume a small job shop with four turning machines processing brass parts and a 7.5 HP rotary screw CAS with the start/stop mode

providing compressed air for machining purposes. Figure 5 shows the layout of the production system. The 7.5 HP CAS is rated as 21 cfm at 150 psig with a motor efficiency of 91%. The interarrival time of the parts is exponentially distributed with an average of 10 min. The processing amount (A) is assumed to be fixed for all the machines as 1,841,105 mm³ (see Table 1). We simulate a total of 20 cases considering four different sets of scenarios with five case studies in each simulation set. Except for the cases in Set 2, the machine processing time for all the machines follows a normal distribution with mean = 9 min and standard deviation = 1.8 min (coefficient of variation = 0.2). For each of the simulation sets, the effect of change in the following parameters: the size of the air receiver (V), the total magnitude of compressed air leakages (L_T), pressure setpoints (P_{Start} and P_{Stop}), and machine-level air demand (C_M) on the peak kW of 15-min MA for power demand (P_{kW15}) and total kWh consumption are evaluated. We assume that the facility works for 10 hrs/day and 7 days/week. Therefore to estimate the monthly electricity cost, we simulate 18,600 mins (31 days \times 10 hrs/day \times 60 min = 18,600 min).

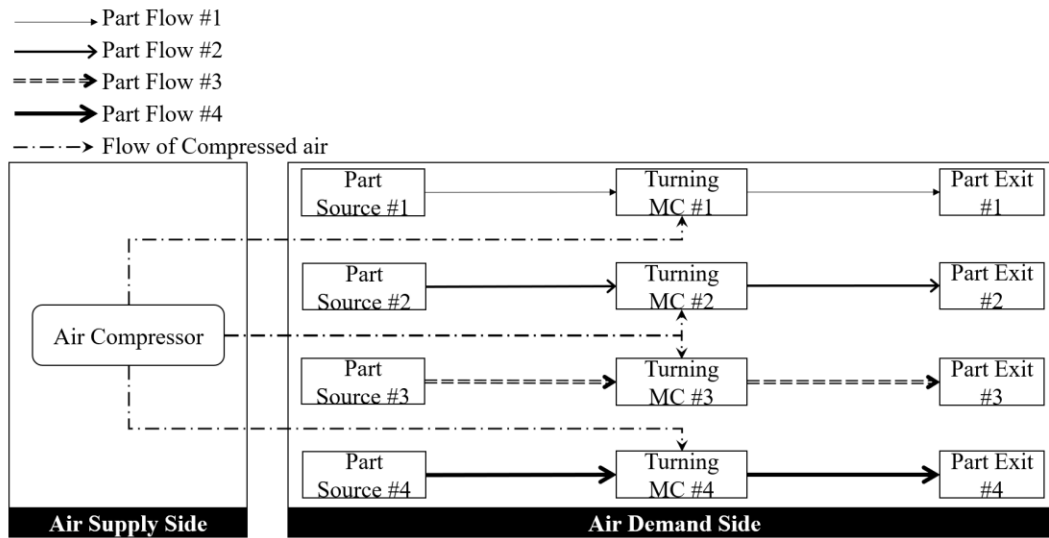


Figure 5. The layout of the production system

Table 3 presents the results from Set 1 of the simulation case study and we define Set 1 as our baseline set. Case 1-1 (C1-1) represents a simulation case with realistic estimations for V , L_T , P_{Stop} , P_{Start} , and C_M with an assumption that the system pressure requirement is 80 psig. C1-2 to C1-5 are counterparts of C1-1 with one different parameter. For C1-2, we double V (60 gals to 120 gals) and observe similar results as compared to C1-1. Since the total air consumption is unchanged, a CAS will have to work for a similar amount of time, and hence, the energy performance measures and energy cost are similar. From C1-1 to C1-3, we increase L_T by 50% (6 cfm to 9 cfm). As L_T increases, a CAS would have to work more as the total air consumption is also increased (can be explained by Eq. (3)). Thus, we see an increase in W_{CAS} , P_{kW15} (CAS and factory), and the total kWh consumption (CAS and factory). Subsequently, the energy cost is increased for higher L_T . When the discharge pressure (P_{Stop}) is increased from 130 psig to 140 psig (C1-1 to C1-4), a CAS will take more time to reach the discharge pressure as S is lower for higher pressure (can be explained by Eq. (3)). So, W_{CAS} is higher as compared to C1-1. Subsequently, the total kWh consumed (CAS and factory) and energy cost are higher than C1-1. For C1-5, we simulate a case with a 50% reduction in C_M (4 cfm to 2 cfm), and due to this

change, the total air demand in the system will reduce. Consequently, a CAS will be in stop mode for a longer duration (can be explained by Eq. (4)) and W_{CAS} will be lower than C1-1. Therefore, we see a decrease in W_{CAS} , P_{kW15} (CAS and factory), the total kWh consumed (CAS & factory), and the energy costs.

Table 3. Simulation results from Set 1

| Case | V (gal) | L_T (cfm) | P_{Stop} (psig) | P_{Start} (psig) | C_M (cfm) | Results | | | | | | | Energy Cost (\$) | | | |
|-------|------------|----------------|----------------------|-----------------------|----------------|--------------------|-------------------|-------|--------------------|--------|--------------------|--------|------------------|-------|-------|-------|
| | | | | | | CAS | | | Machine | | Factory | | LA | MI | CT | HI |
| | | | | | | P_{kW15} (kW) | W_{CAS} (kW) | kWh | P_{kW15} (kW) | kWh | P_{kW15} (kW) | kWh | | | | |
| C 1-1 | 60 | 6 | 130 | 100 | 4 | 6.43 | 5.66 | 1,754 | 49 | 11,749 | 56 | 13,503 | 1,516 | 1,855 | 3,150 | 5,028 |
| C 1-2 | 120 | 6 | 130 | 100 | 4 | 6.62 | 5.66 | 1,753 | 49 | 11,749 | 55 | 13,502 | 1,514 | 1,853 | 3,146 | 5,022 |
| C 1-3 | 60 | 9 | 130 | 100 | 4 | 6.76 | 6.49 | 2,000 | 50 | 11,746 | 57 | 13,747 | 1,546 | 1,890 | 3,210 | 5,124 |
| C 1-4 | 60 | 6 | 140 | 110 | 4 | 6.76 | 6.08 | 1,884 | 48 | 11,752 | 55 | 13,636 | 1,522 | 1,867 | 3,168 | 5,057 |
| C 1-5 | 60 | 6 | 130 | 100 | 2 | 4.13 | 3.66 | 1,136 | 50 | 11,751 | 54 | 12,887 | 1,455 | 1,776 | 3,018 | 4,818 |

Table 4 (Set 2) shows the simulation results with the machines having an exponentially distributed processing time with mean = 9 mins. All the input parameters corresponding to the rows in Table 4 (Set 2) are similar to the input parameters in Table 3 (Set 1). Since the coefficient of variation for the exponential distribution is 1, the variability in T would be much higher as compared to the normally distributed T (Set 1). So, it is likely that A / T can be higher than Set 1. Hence, P_{kW15} (machine and factory) is observed to be much higher than Set 1 (can be explained by Eq. (12)). This shows a clear increase in demand for exponentially distributed processing time. Subsequently, the energy cost is higher as compared to Set 1.

Table 4. Simulation results from Set 2 (machine processing time is exponentially distributed)

| Case | V (gal) | L_T (cfm) | P_{Stop} (psig) | P_{Start} (psig) | C_M (cfm) | Results | | | | | | | Energy Cost (\$) | | | |
|-------|------------|----------------|----------------------|-----------------------|----------------|--------------------|-------------------|-------|--------------------|--------|--------------------|--------|------------------|-------|-------|-------|
| | | | | | | CAS | | | Machine | | Factory | | LA | MI | CT | HI |
| | | | | | | P_{kW15} (kW) | W_{CAS} (kW) | kWh | P_{kW15} (kW) | kWh | P_{kW15} (kW) | kWh | | | | |
| C 2-1 | 60 | 6 | 130 | 100 | 4 | 6.43 | 5.61 | 1,740 | 80 | 11,745 | 86 | 13,485 | 1,772 | 2,024 | 3,506 | 5,612 |
| C 2-2 | 120 | 6 | 130 | 100 | 4 | 6.62 | 5.69 | 1,763 | 77 | 11,721 | 83 | 13,484 | 1,747 | 2,007 | 3,471 | 5,554 |
| C 2-3 | 60 | 9 | 130 | 100 | 4 | 6.76 | 6.50 | 2,000 | 74 | 11,720 | 80 | 13,720 | 1,746 | 2,021 | 3,487 | 5,579 |
| C 2-4 | 60 | 6 | 140 | 110 | 4 | 6.76 | 6.14 | 1,900 | 77 | 11,722 | 83 | 13,622 | 1,758 | 2,023 | 3,497 | 5,595 |
| C 2-5 | 60 | 6 | 130 | 100 | 2 | 4.13 | 3.65 | 1,132 | 74 | 11,737 | 77 | 12,869 | 1,654 | 1,907 | 3,293 | 5,270 |

Table 5 (Set 3) presents the simulation results with a reduced machine-level air demand (C_M). All the input parameters for each of the cases in Table 5 (Set 3) are similar to the input parameters in Table 3 (Set 1) with C_M decreased by 25% for each of the cases. Since the compressed air demand reduces, a CAS will have to work less. Hence, a CAS will be on start mode for less duration of time and will be on stop mode for a longer duration (can be explained by Eqs. (3) and (4)) as compared to the cases in Table 3 (Set 1). Consequently, W_{CAS} for Set 3 will be lower than Set 1. Thus, P_{kW15} , the total kWh consumption (CAS & factory), and the energy costs for the cases in Set 4 are lower than Set 1. We can also see from Figure 6 that the peaks of 15-min MA for CAS power demand for C1-1 are higher than C3-1.

Table 5. Simulation results from Set 3

| Case | V (gal) | L_T (cfm) | P_{Stop} (psig) | P_{Start} (psig) | C_M (cfm) | Results | | | | | | | Energy Cost (\$) | | | |
|------|------------|----------------|----------------------|-----------------------|----------------|---------|--|--|---------|--|---------|--|------------------|----|----|----|
| | | | | | | CAS | | | Machine | | Factory | | LA | MI | CT | HI |

| | | | | | | P_{kW15} (kW) | W_{CAS} (kW) | kWh | P_{kW15} (kW) | kWh | P_{kW15} (kW) | kWh | | | | |
|-------|-----|---|-----|-----|-----|--------------------|-------------------|-------|--------------------|--------|--------------------|--------|-------|-------|-------|-------|
| C 3-1 | 60 | 6 | 130 | 100 | 3 | 5.60 | 4.91 | 1,522 | 49 | 11,752 | 55 | 13,274 | 1,492 | 1,824 | 3,098 | 4,945 |
| C 3-2 | 120 | 6 | 130 | 100 | 3 | 5.65 | 4.91 | 1,523 | 50 | 11,749 | 55 | 13,272 | 1,493 | 1,825 | 3,100 | 4,949 |
| C 3-3 | 60 | 9 | 130 | 100 | 3 | 6.43 | 5.75 | 1,782 | 49 | 11,749 | 55 | 13,531 | 1,515 | 1,856 | 3,150 | 5,029 |
| C 3-4 | 60 | 6 | 140 | 110 | 3 | 5.99 | 5.29 | 1,639 | 50 | 11,752 | 55 | 13,391 | 1,507 | 1,842 | 3,128 | 4,994 |
| C 3-5 | 60 | 6 | 130 | 100 | 1.5 | 3.84 | 3.17 | 983 | 49 | 11,749 | 52 | 12,732 | 1,429 | 1,749 | 2,970 | 4,741 |

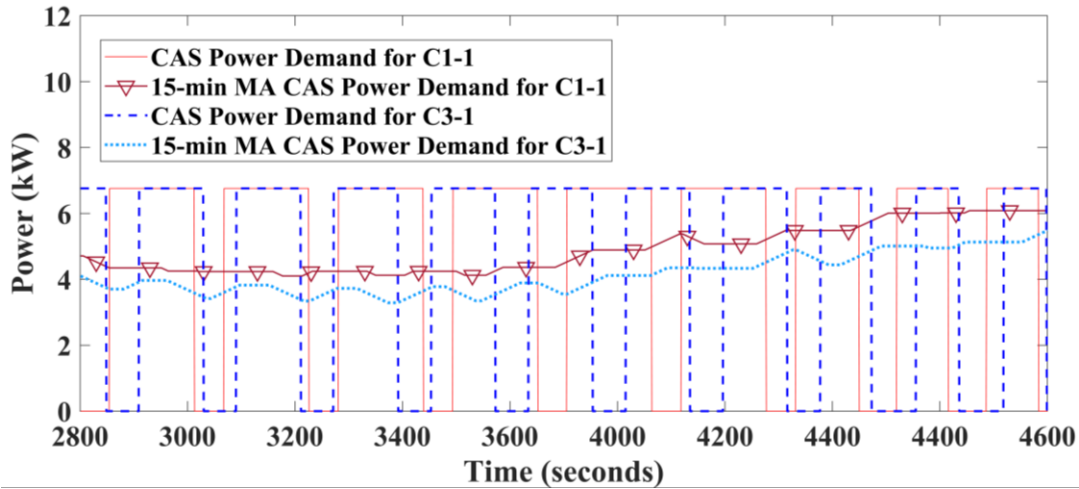


Figure 6. CAS power comparison for C1-1 and C3-1

The simulation results with decreased pressure setpoints are shown in Table 6 (Set 4). The input parameters for each of the cases in Table 6 (Set 4) are similar to the input parameters in Table 3 (Set 1) with a 10 psig reduction in pressure setpoints. As compared to Set 1, a CAS would work for less duration of time on start mode as S is higher for lower pressure (can be explained by Eq. (3)). For example, we can see from the pressure profile provided in Figure 7 that the time taken to reach the discharge pressure of 130 psig (for C1-1) is longer than the time taken to reach the discharge pressure of 120 psig (for C4-1). Also, we can see from Figure 8 that the time duration for the start mode of a CAS for C1-1 is longer than that of C4-1 (see the upper limit of a CAS power profile). Therefore, a CAS would work less as compared to Set 1, and as a result, the total kWh consumption (CAS & factory) and the energy costs for the cases in Set 4 are lower than Set 1.

Table 6. Simulation results from Set 4

| Case | V (gal) | L_T (cfm) | P_{Stop} (psig) | P_{Start} (psig) | C_M (cfm) | Results | | | | | | | Energy Cost (\$) | | | |
|-------|--------------|----------------|----------------------|-----------------------|----------------|--------------------|-------------------|-------|--------------------|--------|--------------------|--------|------------------|-------|-------|-------|
| | | | | | | CAS | | | Machine | | Factory | | LA | MI | CT | HI |
| | | | | | | P_{kW15} (kW) | W_{CAS} (kW) | kWh | P_{kW15} (kW) | kWh | P_{kW15} (kW) | kWh | | | | |
| C 4-1 | 60 | 6 | 120 | 90 | 4 | 5.77 | 5.22 | 1,620 | 49 | 11,747 | 54 | 13,367 | 1,497 | 1,834 | 3,112 | 4,968 |
| C 4-2 | 120 | 6 | 120 | 90 | 4 | 6.09 | 5.23 | 1,620 | 49 | 11,752 | 55 | 13,372 | 1,500 | 1,836 | 3,117 | 4,976 |
| C 4-3 | 60 | 9 | 120 | 90 | 4 | 6.47 | 6.00 | 1,859 | 49 | 11,754 | 56 | 13,613 | 1,526 | 1,869 | 3,172 | 5,064 |
| C 4-4 | 60 | 6 | 130 | 100 | 4 | 6.43 | 5.66 | 1,754 | 49 | 11,749 | 56 | 13,503 | 1,516 | 1,855 | 3,150 | 5,028 |
| C 4-5 | 60 | 6 | 120 | 90 | 2 | 3.64 | 3.38 | 1,048 | 50 | 11,753 | 54 | 12,801 | 1,448 | 1,766 | 3,001 | 4,791 |

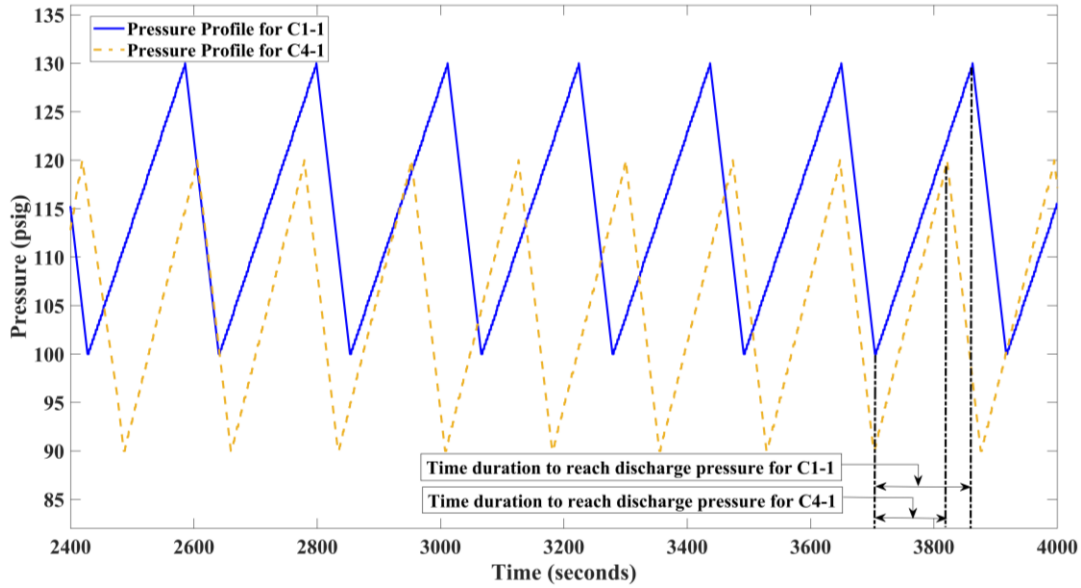


Figure 7. Pressure profile comparison for C1-1 and C4-1

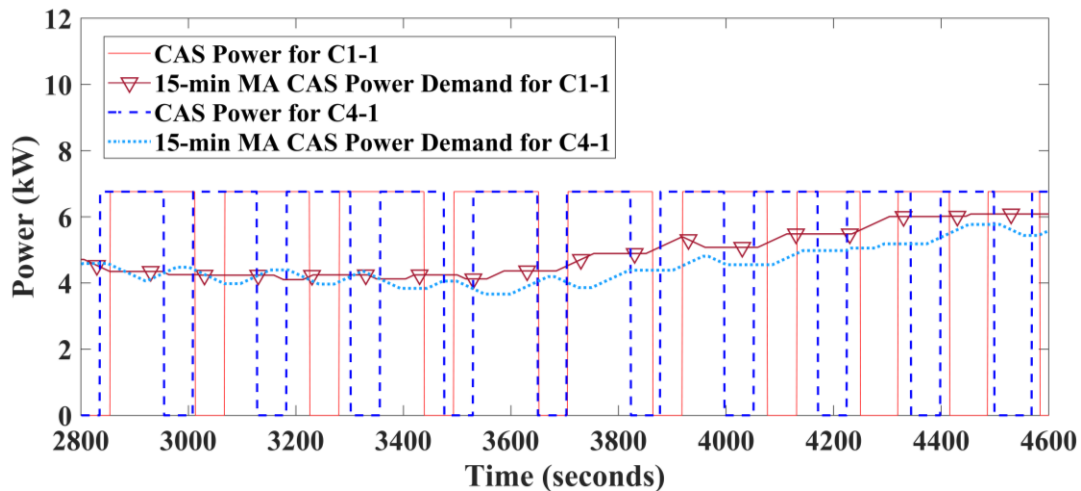


Figure 8. CAS power comparison for C1-1 and C4-1

5. Conclusions

A pressure-discretized energy simulation model for a rotary screw CAS with the start/stop controls integrated with the turning machines to estimate the energy cost for a manufacturing system is proposed in this paper. The simulation model presented in the paper considers various operational parameters for a CAS and turning machines to provide the peak kW of the MA for power demand and the total kWh consumed. The results from the simulation examples show that the magnitude of compressed air leakage, discharge pressure, machine-level compressed air consumption, and the variability of machine processing time is a significant factor that affects the energy performance measures and energy cost. Additionally, the size of the air receiver was found to have a limited impact on the peak kW, total kWh consumption, and energy cost. Overall, the manufacturers can reduce their energy costs by reducing the

compressed air leakages, discharge pressure, and the variability of processing time. Thus, we believe that the results from the proposed simulation model can help the manufacturers in reducing their energy costs by choosing optimal parameters for a CAS and machines. Additionally, by improving the energy consumption of the manufacturing system, the manufacturers can contribute to the reduction of carbon footprint. Even though this study provides a useful simulation tool for reducing energy costs, it does not consider the pressure drop across the distribution system, and we expect to address this in the future study.

References

- CAGI. 2016. *Compressed Air and Gas Handbook*. 6th ed. Compressed Air and Gas Institute, Ohio.
- Compressed Air Challenge. 2002. "Fundamentals of Compressed Air Systems." *US Department of Energy*.
- Diaz, N., E. Redelsheimer, and D. Dornfeld. 2011. "Energy Consumption Characterization and Reduction Strategies for Milling Machine Tool Use." In *J. Hesselbach, C. Herrmann (Eds.), Globalized Solutions for Sustainability in Manufacturing, Springer*, 263–67. Berlin Heidelberg.
- Downs, Chris. 2020. "The Relationship Between Pressure and Flow in a Compressed Air System." *Compressed Air Best Practices*. <https://www.airbestpractices.com/system-assessments/pressure/relationship-between-pressure-and-flow-compressed-air-system>.
- Gutowski, T.G., M.S. Branham, J.B. Dahmus, A.J. Jones, A. Thirez, and D.P. Sekulic. 2009. "Thermodynamic Analysis of Resources Used in Manufacturing Processes." *Environ. Sci. Technol.* 43: 1584–90.
- Herrmann, C., S. Thiede, S. Kara, and J. Hesselbach. 2011. "Energy Oriented Simulation of Manufacturing Systems –Concept and Application." *CIRP Ann. - Manuf. Technol.*, no. 60: 45–48.
- Jeon, H.W., S. Lee, A. Kargartan, and Y. Kang. 2017. "Power Demand Risk Models on Milling Machines." *Journal of Cleaner Production*, no. 165: 1215–28.
- Jeon, H.W., Seokgi Lee, and Chao Wang. 2019. "Estimating Manufacturing Electricity Costs by Simulating Dependence between Production Parameters." *ROBOT CIM-INT MANUF*, no. 55: 129–40.
- Jeon, H.W., and S.G. Lee. 2016. "Manufacturing Energy Consumption Model for Product Mix and Design." In *Proceedings of the Sixth International Conference on Flexible Automation and Intelligent Manufacturing (FAIM)*. Seoul, Republic of Korea.
- Jeon, H.W., M. Taisch, and V. Prabhu. 2016. "Measuring Variability on Electrical Power Demands in Manufacturing Operations." *Journal of Cleaner Production*, no. 137: 1628–46.

- Kara, S., and W. Li. 2011. "Unit Process Energy Consumption Models for Material Removal Processes." *CIRP Annals - Manufacturing Technology*, no. 60: 37–40.
- LBNL, and RDC. 2003. *Improving Compressed Air System Performance-a Sourcebook for Industry*. Third. US DOE.
<https://www.energy.gov/sites/prod/files/2016/03/f30/Improving%20Compressed%20Air%20Sourcebook%20version%203.pdf>.
- Li, Y., Y. He, Y. Wang, Y. Wang, P. Yan, and S. Lin. 2015. "A Modeling Method for Hybrid Energy Behaviors in Flexible Machining Systems." *Energy* 86: 164–74.
- Saidur, R., N.A. Rahim, and M. Hasanuzzaman. 2010. "A Review on Compressed-Air Energy Use and Energy Savings." *Renewable and Sustainable Energy Reviews*, no. 14: 1135–53.
- Schmidt, Chris, and JK Kissock. 2003. "Power Characteristics of Industrial Air Compressors."
———. 2005. "Modeling and Simulation of Air Compressor Energy Use." In *ACEEE Summer Study on Energy Efficiency in Industry*, 1:131–42. 13.
- Senniappan, A.P. 2004. "Baselining a Compressed Air System—an Expert Systems Approach." MS thesis, Morgantown, USA: West Virginia University.
- Shanghai, H.Q., and A. McKane. 2008. "Improving Energy Efficiency of Compressed Air System Based on System Audit." *LBNL*.
- "State Electricity Profiles - Energy Information Administration (n.d.)." 2017.
<https://www.eia.gov/electricity/state/>.
- "U.S. Energy Information Administration (EIA)." 2019. Accessed May 9.
<https://www.eia.gov/energyexplained/use-of-energy/industry.php>.
- Vechev, S., I. Kolev, K. Ivanov, and S. Gechevski. 2014. "Empirical Models for Specific Energy Consumption and Optimization of Cutting Parameters for Minimizing Energy Consumption during Turning." *Journal of Cleaner Production*, no. 80: 139–49.
- Wang, Yong, and Lin Li. 2015. "Time-of-Use Electricity Pricing for Industrial Customers: A Survey of U.S. Utilities." *Applied Energy*, no. 149: 89–103.